Catalysis Today 164 (2011) 124–130

Contents lists available at ScienceDirect

Catalysis Today

journal homepage: www.elsevier.com/locate/cattod

# Specific tuning of acid/base sites in apatite materials to enhance their methanol thiolation catalytic performances

Carole Lamonier[a,*], Jean-François Lamonier[a], Belaïd Aellach[b], Abdelaziz Ezzamarty[b], Jacques Leglise[c]

[a] Unité de Catalyse et de Chimie du Solide, UMR CNRS 8181, Université des Sciences et Technologies de Lille, 59655 Villeneuve d'Ascq, France
[b] Laboratoire de Catalyse Hétérogène, Université Aïn Chock, Casablanca, Morocco
[c] Ministère de l'Enseignement supérieur et de la recherche, 1 rue Descartes, 75005 Paris, France

ARTICLE INFO

*Article history:*
Available online 4 November 2010

*Keywords:*
Hydroxyapatite
Carbonated hydroxyapatite
Acidic and basic catalysts
Methanol conversion
Thiolation

ABSTRACT

Calcium hydroxyapatites (Hap) solids were prepared with various Ca/P atomic ratios, leading to stoichiometric $Ca_{10}(PO_4)_6(OH)_2$, calcium-deficient (Ca/P < 1.67) and calcium-rich materials. Their acid/base properties were tailored by the introduction of sodium and/or carbonate entities. The various hydroxyapatite solids were characterized by chemical analysis, IR, XRD and TGA techniques, and tested in methanol thiolation. The acid/base properties were evaluated using the isopropanol decomposition as a test reaction. Catalytic performances were found to be related to their acid/base properties. Total methanol conversion at 400 °C with high selectivity in methanethiol (60%) was obtained for the Na-$CO_3$ modified Hap.



## 1. Introduction

Thiochemistry is related to the synthesis of more than 30 compounds such as mercaptans, sulphides, sulphones, sulphoxides, thioacids and thioesters. Among them, mercaptans are one of the most important class of compounds because they are often used as starting materials for the synthesis of other thiocompounds [1]. Methanethiol, $CH_3SH$, also referred as methylmercaptan is produced in large amount because of its utilization in the first step of the commercial synthesis of methionine, an amino acid used as poultry feed supplement [1]. Industrially, methanethiol is currently prepared by direct thiolation of methanol over salts or oxides of alkali metals supported on alumina or acidic supports. Its synthesis from $CH_3OH$ and $H_2S$ needs a catalyst with high activity but also high selectivity since other products can also been formed, specially, $CH_3SCH_3$. According to Folkins and Miller [2], efficient catalysts for methanethiol conversion (80–90% selectivity at 350–420 °C) are alkali metal oxides or alkali metal carbonates deposited on alumina. Mashkina et al. [3] reported also that transition-metal oxides were more efficient when they are supported on alumina than on silica or silica-alumina. Indeed, the reaction between methanol and hydrogen sulphide involves acidic and basic sites. Mashkina et al. [4] have stated that the presence of basic sites can favor the formation of methanethiol, because methanethiol transforms to dimethylsulphide ($CH_3SCH_3$) if medium basic sites are close to strong Lewis acid sites (pairs of acid and base centers). Lavalley and coworkers [5] have studied various metals oxides ($TiO_2$, $ZrO_2$, $Al_2O_3$, MgO, ...) as catalysts for methanol thiolation and found that the fewer the amount of basic sites, the higher was the selectivity to dimethylsulphide. Moreover, they showed that the highest basicity of MgO led to the lowest activity but also to a selective formation of methanethiol [5]. However, activity and selectivity did not appear to be simply related to basicity or acidity. Indeed, pairs of Lewis acid and base centers are involved in the reaction between methanol and $H_2S$ [5]. More recently, El Ouassouli et al. [6] have reported that transition-metal sulphides supported on hydroxyapatite transform selectively dimethyldisulphide ($CH_3SSCH_3$) into $CH_3SH$, which was not the case when the metal sulphides were supported on alumina. This was explained by the presence of weaker acidic and basic Lewis sites on hydroxyapatite compared to alumina [6].

Calcium hydroxyapatites (Hap), with structural formula $Ca_{10}(PO_4)_6(OH)_2$ are handled as harmless solids to environment, they are thermally very stable and almost not soluble in water. When prepared under mild conditions, Hap can have interesting specific surface areas and porous volumes for catalysis purpose [7]. Moreover, their flexible structure allows the presence of defects, which can be obtained by ion substitution at either cationic or anionic sites [8].

In this work, we take advantage of this remarkable property to synthesize stoichiometric (Ca/P molar ratio = 1.67), calcium-deficient (Ca/P < 1.67) and calcium-rich (Ca/P > 1.67) apatites. The acid–base surface properties have been tailored introducing $Na^+$ or $CO_3^{2-}$ ions in the Hap structure during the preparation proce-

* Corresponding author. Tel.: +33 3 20 33 77 33; fax: +33 3 20 43 65 61.
*E-mail address:* carole.lamonier@univ-lille1.fr (C. Lamonier).

0920-5861/$ – see front matter © 2010 Elsevier B.V. All rights reserved.
doi:10.1016/j.cattod.2010.10.035

dure. Characterizations (XRD, IR, TGA) have been performed and acid/base properties have been evaluated from the isopropanol decomposition reaction [9]. The catalysts, containing both acidic and basic centers of various strengths, have been tested in methanol thiolation.

## 2. Experimental

### 2.1. Catalysts preparation

All syntheses were carried out by the coprecipitation method. An aqueous solution of calcium nitrate (0.167 mol $L^{-1}$) was added dropwise for 3 h at around 100 °C to a solution of $(NH_4)_2HPO_4$ (0.1 mol $L^{-1}$) while stirring, the Ca/P molar ratio being equal to 1.67. The solution was adjusted to pH 10, by adding an ammonia solution. The resulting precipitate was slowly filtered, washed with hot water, dried under vacuum at 80 °C and calcined at 400 °C. Stoichiometric hydroxyapatite $Ca_{10}(PO_4)_6(OH)_2$ (Hap) was then obtained. With the same procedure, calcium-deficient hydroxyapatite (HapD) with a general formula $Ca_{10-x}(HPO_4)_x(PO_4)_{6-x}(OH)_{2-x}$, where $x$ represents cationic vacancies [10,11], was obtained adjusting the calcium nitrate concentration to obtain a solution with an Ca/P molar ratio equal to 0.9. As already reported, the Ca/P atomic ratio of the precipitate Hap did not match that of the solution of the initial reagents [12,13].

Sodium ions were introduced during the preparation procedure using a sodium nitrate precursor, dissolved in the calcium nitrate solution, the (Ca + Na)/P molar ratio was fixed to 1.67 for the synthesis of sodium-doped stoichiometric hydroxyapatite (Hap-Na) and to 0.9 for Ca-deficient hydroxyapatite (HapD-Na).

Stoichiometric carbonated hydroxyapatites (Hap-$CO_3$) and solids containing sodium ions (Hap-Na-$CO_3$) were obtained using the same coprecipitation procedure, but in which the Ca (+Na)/P molar ratio in the solution was fixed to 2. In this case, carbonate groups provided from atmospheric $CO_2$ could be introduced in the Hap structure [14].

Ca-rich hydroxyapatites (HapE) were also synthesized using a solution of $(NH_4)_2HPO_4$ (0.1 mol $L^{-1}$) added dropwise to a calcium solution (0.55 mol $L^{-1}$) while stirring, with an Ca/P molar ratio equal to 5.5. This high ratio allowed to introduce carbonate ions in the synthesized stoichiometric hydroxyapatite. The corresponding catalyst was denoted HapE-$CO_3$.

More carbonate ions were also introduced in an Ca-rich hydroxyapatite using sodium carbonate (5.83 g) dissolved in the ammonium hydrogenophosphate solution (0.1 mol $L^{-1}$). In this case, the resulting apatite was denoted HapE-Na-$CO_3$.

### 2.2. Characterization techniques

Chemical analysis was performed by the "Service Central d'Analyses du CNRS" (Vernaison, France).

TGA analyses were performed using a Thermal Analysis instrument (Model SDT 2960) on 20 mg of sample. Mass losses were recorded under synthetic air, with a heating rate of 4 °C $min^{-1}$ from 20 °C to 800 °C.

The specific surface area of the catalysts was measured by $N_2$ physisorption using the BET method on a Quantasorb junior apparatus. A mass around 100 mg of sample was degassed at 150 °C for 45 min before measurements.

The crystal structure of solids was performed by X-ray diffraction (XRD) technique with a Siemens D5000 diffractometer equipped with a copper anode. The data were collected at 20 °C with a step size of 0.02° and a step time equal to 1.5 s. The patterns were collected over the $2\theta$ range from 10° to 80°.

Transmission infrared (IR) spectra were recorded from 200 $cm^{-1}$ to 4000 $cm^{-1}$, at room temperature, on a Nicolet 460 spectrophotometer. Samples were prepared by mixing 1 mg of powdered solid with 150 mg of dried KBr.

Catalytic tests were performed at 400 °C at atmospheric pressure (101.13 kPa) in an U-glass reactor filled with 200 mg of catalysts under a continuous flow of reactants: $CH_3OH$ (4 $cm^3$ $mn^{-1}$) and $H_2S$ (4 $cm^3$ $mn^{-1}$) diluted in $CH_4$ (4 $cm^3$ $mn^{-1}$). $H_2S$ and $CH_4$ came from the decomposition at 400 °C of a flow of $CH_3SSCH_3$ on an $NiMoP/Al_2O_3$ catalyst (Axens, HR348), before mixing with the $CH_3OH$ flow. $CH_3SSCH_3$ and methanol, were fed by bubbling hydrogen through saturators which temperature was fixed at 6 °C and 0 °C respectively. Reactant $CH_3OH$ and products ($CH_3SH$ and $CH_3SCH_3$) were analyzed using a gas chromatograph equipped with a flame ionization detector (FID).

$f$, the conversion, was calculated using the following equation:

$$f = \frac{a_{CH_3SH} + 2a_{CH_3SCH_3}}{a_{CH_3SH} + 2a_{CH_3SCH_3} + a_{CH_3OH}}$$

where $a_y$ is the concentration of $y$.

Calculation formulae for methathiol selectivity $s$:

$$s = \frac{a_{CH_3SH}}{a_{CH_3SH} + 2a_{CH_3SCH_3}}$$

where $a_{CH_3SH}$ and $a_{CH_3SCH_3}$ are the methanethiol and dimethylsulphide concentration respectively.

Acid/base performances of the various catalysts (100 mg) were evaluated using the isopropanol decomposition reaction at 275 °C. The catalytic reaction was carried out under inert atmosphere in a continuous-flow pyrex microreactor at atmospheric pressure. The feed was obtained by bubbling the argon (12 $cm^3$ $mn^{-1}$) through liquid isopropanol in a saturator at 0 °C. Products (propene, acetone and diisopropylether) were analyzed by gas chromatography equipped with an FID detector.

## 3. Results and discussion

Chemical composition values (Table 1) were found to be in agreement with the formation of an Ca-deficient apatite for HapD and HapD-Na solids, since the corresponding Ca/P ratios were found to be equal to 1.56 and 1.54 respectively, *i.e.* lower than the 1.67 value expected for a stoichiometric hydroxyapatite $Ca_{10}(PO_4)_6(OH)_2$. From chemical analysis, the number $x$ of vacancies in the Ca-deficient HapD apatite, $Ca_{10-x}(HPO_4)_x(PO_4)_{6-x}(OH)_{2-x}$, [13,15], could be determined as 0.64 vacancy per 10 calcium ions. The Ca/P atomic ratios (rang-

**Table 1**
Chemical composition results and surface area of the hydroxyapatite materials.

| Catalysts | Ca (wt.%) | P (wt.%) | Na (wt.%) | C (wt.%) | Ca/P (at./at.) | Specific surface area ($m^2$ $g^{-1}$) |
|---|---|---|---|---|---|---|
| HapD | 39.24 | 19.40 | – | – | 1.56 | 81 |
| HapD-Na | 38.85 | 19.49 | 0.44 | – | 1.54 | 78 |
| Hap | 37.10 | 17.45 | – | – | 1.64 | 79 |
| Hap-Na | 41.00 | 19.31 | 0.61 | – | 1.64 | 77 |
| Hap-$CO_3$ | 39.10 | 18.45 | – | 0.33 | 1.63 | 107 |
| Hap-Na-$CO_3$ | 38.10 | 18.30 | 0.52 | 0.33 | 1.60 | 106 |
| HapE-$CO_3$ | 37.03 | 15.04 | 0 | 1.3 | 1.9 | 76 |
| HapE-Na-$CO_3$ | 34.96 | 12.58 | <0.02 | 2.9 | 2.1 | 77 |

**Table 2**
Lattice parameters a and c obtained for Hap materials from XRD patterns.

| Catalysts | $a$ (±0.0002) nm | $c$ (±0.0002) nm |
|---|---|---|
| HapD | 0.9423 | 0.6881 |
| HapD-Na | 0.9420 | 0.6889 |
| Hap | 0.9427 | 0.6886 |
| Hap-Na | 0.9426 | 0.6894 |
| Hap-$CO_3$ | 0.9436 | 0.6886 |
| Hap-Na-$CO_3$ | 0.9434 | 0.6881 |
| HapE-$CO_3$ | 0.9416 | 0.6887 |
| HapE-Na-$CO_3$ | 0.9407 | 0.6885 |

ing between 1.60 and 1.64) of the Hap, Hap-Na, Hap-$CO_3$ and Hap-Na-$CO_3$ solids were found to be slightly lower than the stoichiometric value. In both samples HapE-$CO_3$ and HapE-Na-$CO_3$, the Ca/P atomic ratio was found to be close to 2, and their $CO_3^{2-}$ content very high (Table 1). According to the literature data [16,17], carbonate ions can be hosted at two different sites: at site A, where $CO_3^{2-}$ ions, substitute for $OH^-$ ions, and at site B, where they replace $PO_4^{3-}$ ions. A-type and B-type can be distinguished on the basis of their IR spectra. An A-type carbonated Hap derived from stoichiometric Hap $Ca_{10}(PO_4)_6(OH)_{2-2x}(CO_3)_x$ (Ca/P = 1.67) with creation of anionic ($OH^-$) vacancies [14], whereas an B-type carbonated Hap has a general composition as $Ca_{10-x}(PO_4)_{6-x}(CO_3)_x(OH)_{2-x}$ where $PO_4^{3-}$ ions are substituted by $CO_3^{2-}$ ions with creation of $x$ cationic ($Ca^{2+}$) and $x$ anionic ($OH^-$) vacancies to ensure electroneutrality [18], the Ca/P ratio has been reported, for B-type carbonated Hap, to be above 1.67. Thus, the Ca/P values of the HapE-$CO_3$ and HapE-Na-$CO_3$ solids, which were found to exceed largely 1.67, suggest the formation of an B-type carbonated apatite in these solids. Moreover, it is noticeable for HapE-Na-$CO_3$, that though carbonate was coming from sodium carbonate in solution, only few calcium ions were substituted by sodium ions (<0.02 wt.%, Table 1).

Specific surface areas of all the calcined apatite materials were found to be close to 80 $m^2\,g^{-1}$ excepting for the two Hap(-Na)-$CO_3$ solids, for which the specific surface area reached 106–107 $m^2\,g^{-1}$ (Table 1). The specific surface area of all carbonated apatite materials were thus found to be rather high in comparison with the values reported in literature [19,20]. Indeed, Padilla et al. [19] have shown that the hydroxyapatite specific surface area was very sensitive to the presence of $CO_2$ during the synthesis, leading to introduction of carbonate ions in the apatite structure. Hence, high specific surface areas in our samples could reveal the presence of structural carbonate groups. However, a too high content of carbonate groups might suppress such beneficial effect on textural properties, since lower specific surface area values were observed for both HapE-$CO_3$ and HapE-Na-$CO_3$.

Fig. 1 shows the XRD patterns of the apatite solids, only HapD and HapD-Na XRD patterns are shown as examples. All solids, calcined at 400 °C, were composed of crystalline hydroxyapatite (JCPDS 01-086-074), no other crystalline phase could be detected in all samples. Hydroxyapatite crystallized in the hexagonal $P6_3/m$ space group and lattice parameters $a$ and $c$, reported in Table 2, were determined using (0 0 2) and (3 0 0) reflections. The calculated lattice parameters of Hap are $a = b = 0.9427$ nm and $c = 0.6886$ nm. The $c$ value showed a slight increase with addition of sodium in Hap-Na. A same trend is observed comparing the $c$-axis values of HapD and HapD-Na. This increase in $c$-axis values leading to the expansion in cell volume has been already reported by Kannan et al. [21] for all sodium-substituted apatites when compared to pure Hap. High amounts of carbonate ions in HapE-$CO_3$ and HapE-Na-$CO_3$ (1.3 and 2.9 wt.% of C) resulted in a decrease in the $a$-axis values and this behavior can be explained by considering that the carbonate ion reduced the $a$-axis when replacing the phosphate ion, confirming

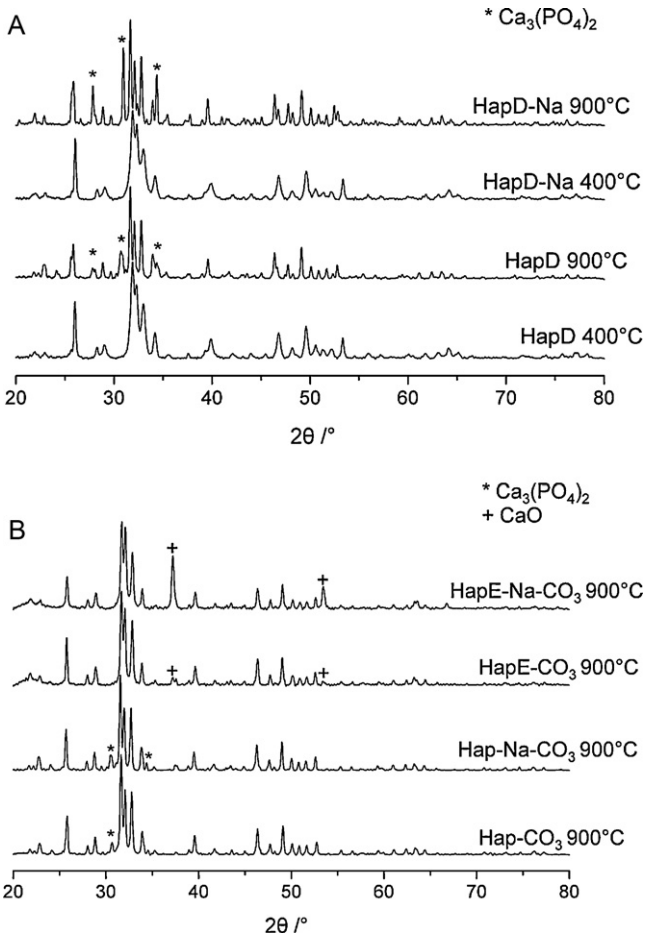


**Fig. 1.** Diffraction patterns of (A) HapD and HapD-Na calcined at 400 °C and 900 °C and (B) Hap-$CO_3$, Hap-Na-$CO_3$, HapE-$CO_3$, HapE-Na-$CO_3$ calcined at 900 °C.

that carbonate ion enters the apatitic structure in site B [22]. The crystallinity of all materials was found to increase with calcination temperature, and major differences in XRD patterns could be observed after calcination above 700 °C. XRD patterns of samples HapD and HapD-Na that have been calcined at 900 °C are shown in Fig. 1. The formation of a new crystallized phase is clearly evidenced. The new reflections, marked with * in Fig. 1, are assigned to an $Ca_3(PO_4)_2$ phase (JCPDS 09-0169), such a phase was observed for all HapD and Hap solids, containing or not sodium or carbonate ions. Besides, no evidence of an $Na_2O$ phase was found in the Na-containing samples, which might be expected because of the low sodium content (≤0.61 wt.%) of those materials (Table 1).

The formation of an $Ca_3(PO_4)_2$ phase result presumably from the transformation of the initial calcium-deficient apatite structure into a stoichiometric hydroxyapatite, according the following equation [23]:

$$Ca_{10-x}(HPO_4)_x(PO_4)_{6-x}(OH)_{2-x} \rightarrow (1-x)Ca_{10}(PO_4)_6(OH)_2 + 3x\,Ca_3(PO_4)_2 + xH_2O \quad (1)$$

As observed in Fig. 1, the higher was the quantity $x$ of $HPO_4^-$ ions, the better was the crystallinity of the calcium phosphate phase.

For the Ca-rich apatite materials HapE-$CO_3$ and HapE-Na-$CO_3$ (Fig. 1B), the XRD patterns of the samples calcined at 900 °C were characteristic of an Hap phase, but they also exhibited two XRD peaks (marked with +) ascribed to an CaO phase (JCPDS 00-001-1160). This result could be explained by the thermal decomposition of the B-type carbonated apatite into stoichiometric Hap and CaO

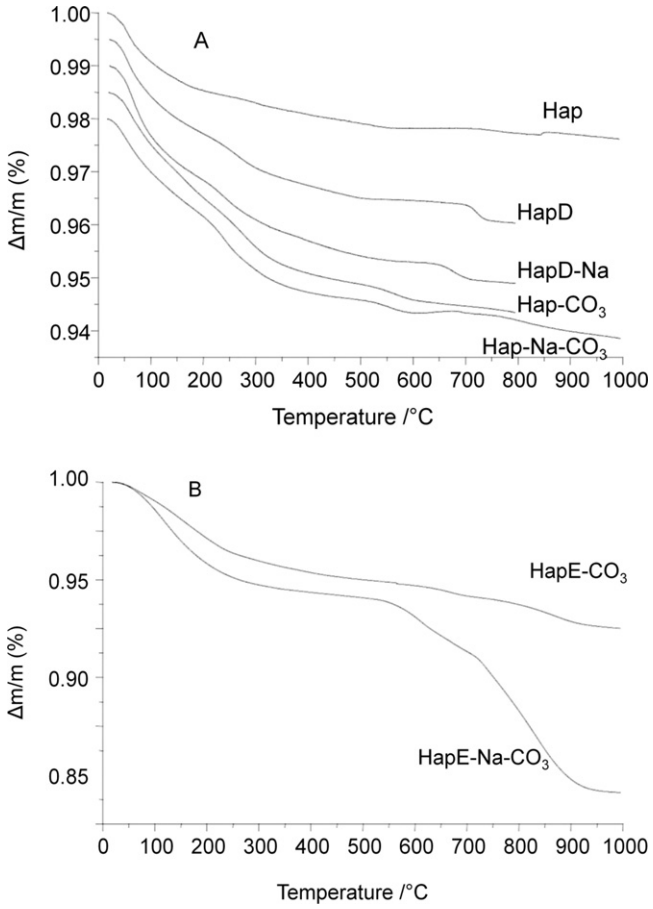


**Fig. 2.** TGA curves of (A) Hap, HapD, HapD-Na, Hap-$CO_3$ and Hap-Na-$CO_3$, and (B) of HapE-$CO_3$ and HapE-Na-$CO_3$.

[18] according the following equation:

$$6Ca_{10-x}(PO_4)_{6-x}(CO_3)_x(OH)_{2-x} + 2x\,H_2O \rightarrow (6-x)Ca_{10}(PO_4)_6(OH)_2 + 4x\,CaO + 6x\,CO_2 \quad (2)$$

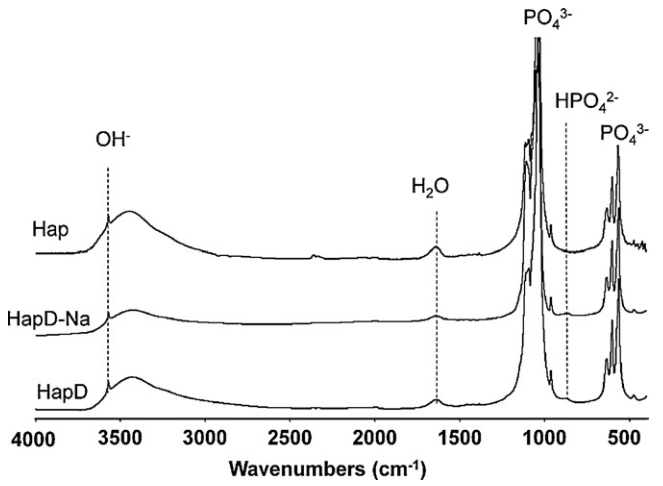


**Fig. 3.** IR spectra of Hap, HapD, HapD-Na.

The thermal decomposition data are shown in Fig. 2. As already reported [15], the weight loss of an Hap solid was caused by physisorbed and constitutive $H_2O$ departure until 500 °C, and a plateau was reached beyond. For the HapD and HapD-Na solids, a marked weight loss attributed to $HPO_4^{-}$ condensation into $P_2O_7^{4-}$ [15] was observed at 700 °C and 650 °C respectively, suggesting that the Na-containing solid was less stable than its counterpart. For carbonated apatites Hap-$CO_3$ and Hap-Na-$CO_3$, this condensation could appear at lower temperature (550 °C). In those samples, the weight loss after 700 °C (Fig. 2A) is attributed to the elimination of $CO_2$, Eq. (2). This result was in agreement with TGA profiles obtained for HapE-$CO_3$ and HapE-Na-$CO_3$ (Fig. 2B) showing an important weight loss until 900 °C in particular for HapE-Na-$CO_3$ with the highest carbonate content.

Fig. 3 shows the IR spectra of Hap, HapD and HapD-Na, and Figs. 4 and 5 show the IR spectra of the four solids containing carbonate groups. All the IR spectra confirmed the formation of an apatite phase with the observation of fundamental vibrational mode of $PO_4$ groups at 574 $cm^{-1}$, 609 $cm^{-1}$, 966 $cm^{-1}$ and 1020–1120 $cm^{-1}$ [16,17]. The presence of adsorbed water could

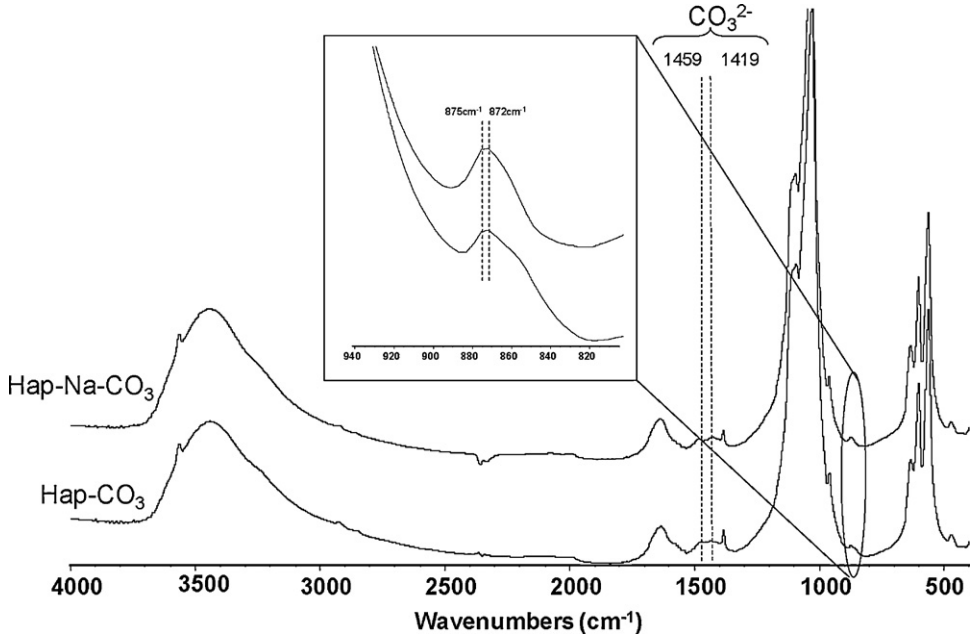


**Fig. 4.** IR spectra of Hap-$CO_3$ and Hap-Na-$CO_3$.

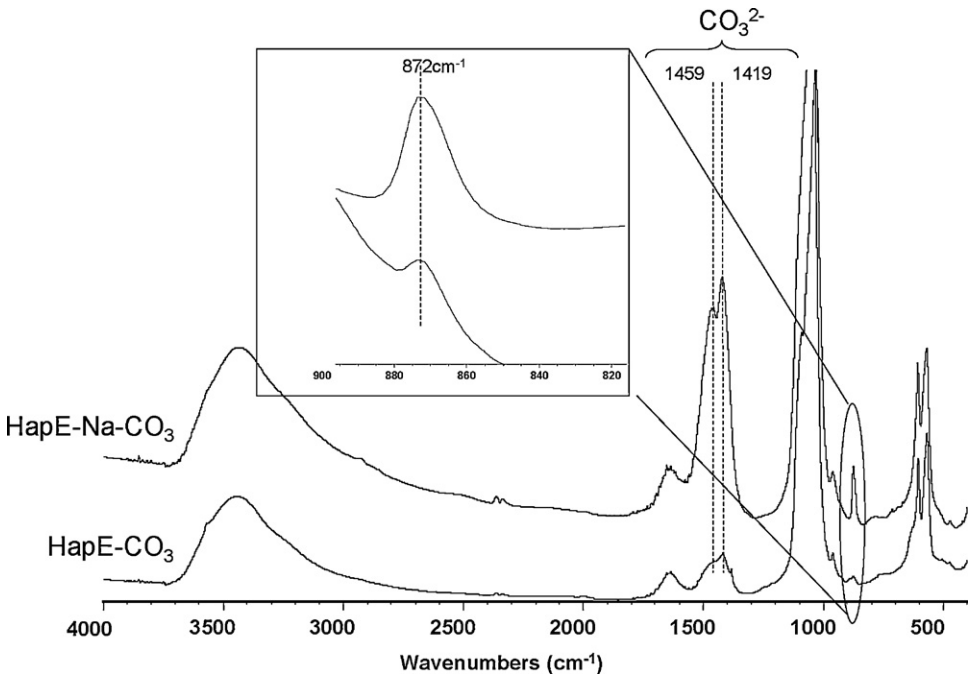


**Fig. 5.** IR spectra of HapE-$CO_3$ and HapE-Na-$CO_3$.

also be detected from IR spectra in the range 3300–3600 $cm^{-1}$ and at about 1637 $cm^{-1}$. In solids based on stoichiometric and deficient Hap, the bands at 633 $cm^{-1}$ and 3572 $cm^{-1}$, shown in Figs. 3 and 4, were attributed to structural OH groups in a hydroxyapatite phase $Ca_{10}(PO_4)_6(OH)_2$ in agreement with results reported in the literature [14,15]. Such OH groups were not detected in Ca-rich samples or in a very low quantity in the case of the HapE-$CO_3$ sample (Fig. 5). This observation was in agreement with the formation of $OH^-$ vacancies in these carbonated apatites as reported by Fleet and Liu [24]. The formation of an A-type carbonated apatite with a general formula $Ca_{10}(PO_4)_6$ $(CO_3)_x(OH)_{2-2x}$ can also lead to a low content of OH groups but cannot explain why the Ca/P ratio of the HapE-$CO_3$ solid was largely above 1.67. Moreover, the bands at 1419 $cm^{-1}$ and 1459 $cm^{-1}$ were attributed to carbonate groups located in sites B substituting $PO_4^{3-}$ groups, they were not assigned to carbonate groups in sites A, which are characterized with IR bands at 1450 $cm^{-1}$ and 1545 $cm^{-1}$ [23]. The band at 875 $cm^{-1}$, characteristic to $HPO_4^{2-}$ groups of an Ca-deficient apatite [10,11], was noticed in Fig. 3 for calcium-deficient apatite and was not detected in the stoichiometric Hap sample. Furthermore, a magnification of the spectral range 800–900 $cm^{-1}$ in Fig. 5 allows to observe a band at 872 $cm^{-1}$ attributed to $CO_3^{2-}$ in site B [24] in the case of HapE-Na-$CO_3$ and HapE-$CO_3$, the intensity of this band being correlated to the carbon content [22]. For Hap-Na-$CO_3$ and Hap-$CO_3$ solids, this band was found to be broader and the presence of a shoulder was observed (Fig. 4). This is attributed to carbonate groups in site B, but also to the presence of $HPO_4^{2-}$ groups detected at 872 $cm^{-1}$ and 875 $cm^{-1}$ respectively [24,7].

On the basis of IR results, calcium-rich hydroxyapatites, HapE-Na-$CO_3$ and Hap-$CO_3$, are typically B-carbonated Ca-rich apatites, The theoretical carbon content of a pure B-type carbonated apatite $Ca_8(PO_4)_4(CO_3)_2$, is about 3.1% with a Ca/P ratio equal to 2, such values appear to be very close to the ones obtained from chemical analysis (Table 1). The Hap-$CO_3$ and Hap-Na-$CO_3$ solids are of a B-carbonated type on slightly Ca-deficient apatite, since the presence of $HPO_4^{2-}$ groups was noticed in those solids. Raman spectroscopy (spectra not shown here) has confirmed the formation of B-carbonated apatites with Raman peaks observed at 1070 $cm^{-1}$ in agreement with literature data [25].

As known in literature [9], the catalytic conversion of isopropanol yields propene, acetone and diisopropylether. With non-carbonated apatite catalysts, diisopropylether was not observed among the reaction products, and with the carbonated catalysts, only a negligible amount of diisopropylether was produced. The apatite solids converted thus isopropanol in propene and acetone. The conversions of isopranol into propene and acetone are shown in Fig. 6. The calcium-deficient apatites HapD and HapD-Na presented

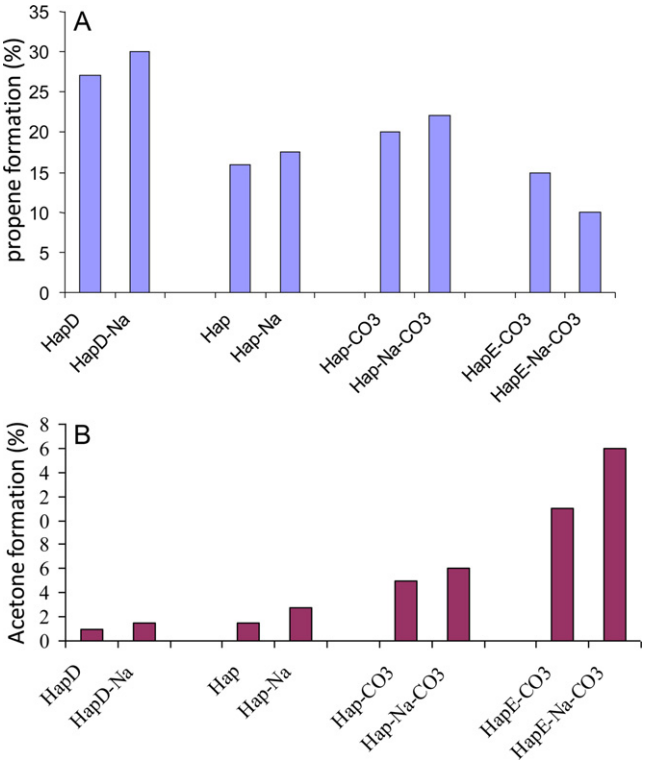


**Fig. 6.** Evaluation of propene (A) and acetone (B) formation from isopropanol decomposition reaction for apatite-based solids.

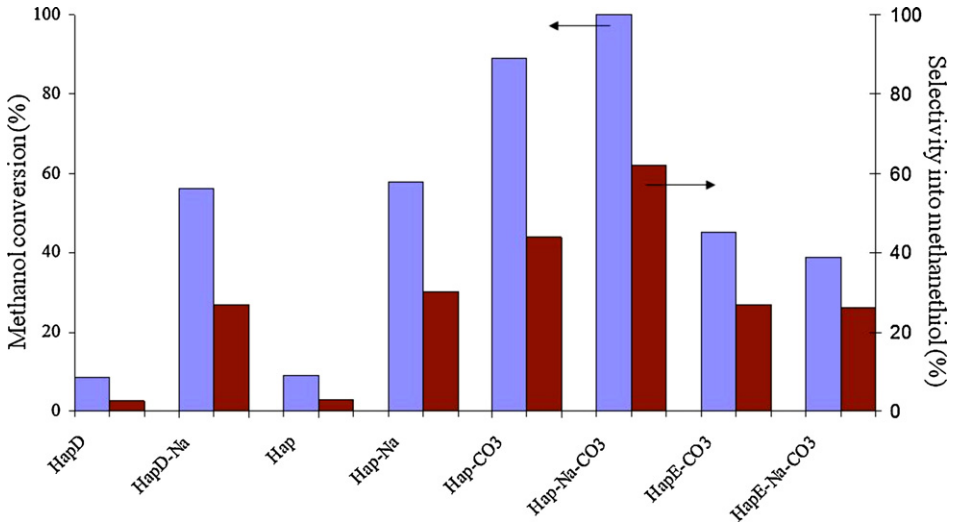


**Fig. 7.** Methanol conversion (%) and selectivity into methanethiol (%) obtained with apatite-based catalysts.

the highest propene formation and the lowest acetone formation, it corresponds to the lowest Ca/P atomic ratio of all investigated apatitic solids. Conversely, the highest acetone formation and the lowest propene formation were obtained on carbonated HapE-Na-$CO_3$ and HapE-$CO_3$ catalysts. Thus, acidic and basic properties of non-stoichiometric Hap appears to be strongly correlated to the Ca/P atomic ratio in the apatitic structure. It implies that basic properties derive from an excess of $Ca^{2+}$ ions and acidic properties from a deficiency of $Ca^{2+}$ions [26]. The presence of $HPO_4^{2-}$ ions, increases the number of acid sites, which explain the higher conversion into propene observed for carbonated Hap-$CO_3$ and Hap-Na-$CO_3$ compared to Hap solids. In addition, it is noticeable that propene formation is slightly favored by the presence of sodium ions in Hap and HapD solids. As exemplified by the conversion levels of isopropanol into acetone, the basicity of Hap-based solids was found to be weak. Fig. 6 showed that it can be adjusted with addition of sodium cations or carbonate anions. Indeed, addition of $Na^+$ ions caused a slight increase in basicity of the deficient, stoichiometric and Ca-rich hydroxyapatites, whereas basicity was largely enhanced upon introduction of $CO_3^{2-}$ ions in stoichiometric Hap and Ca-rich HapE solids.

Thiolation of $CH_3OH$ by $H_2S$ at 400 °C led to the formation of $CH_3SH$ and $CH_3SCH_3$ products, whatever the catalyst used. Hap and HapD catalysts were found to be weakly active as shown in Fig. 7, the conversion of methanol was lower than 10% with those catalysts in agreement with their low basicity. As seen in Fig. 7, Hap and HapD catalysts were also weakly selective into methanethiol; $CH_3SCH_3$ was largely formed on these solids. The presence of sodium and/or carbonate allowed to obtain more selective catalysts. The conversion amounted to 60% when the Hap and HapD solids were doped with sodium ions. Addition of sodium ions enhanced the catalytic performance, because it increases basic properties without decreasing the acidic ones. The Ca-rich carbonated apatite HapE-$CO_3$ converted methanol to more than 40%, and the presence of sodium did not result in an increase of the catalytic performance. Addition of sodium increased the number of basic sites of HapE-$CO_3$, which was characterized by sufficient basic properties coming from carbonate groups, but also decreased its acidic character as deduced from the decrease in propene formation (Fig. 6). HapE-Na-$CO_3$ was then less efficient than his counterpart HapE-$CO_3$. Carbonate addition strongly increased the catalytic performance of Hap, since the methanol conversion increased up to 87%. The simultaneous addition of sodium and carbonate ions led to the most efficient catalyst (100% conversion for Hap-Na-$CO_3$) with a good selectivity in methanethiol (60%) as shown in Fig. 7. A review of Mashkina [27] on the conversion of methanol into methanethiol reported that an active catalyst (bulk oxides catalysts, Na-zeolites, supported acid or alkaline catalysts, . . ..) should ensure in the first place the dissociative chemisorption of methanol with formation of reactive alkoxide groups on the surface. On the surface of a zeolite catalyst, acid OH groups could participate in the interaction of methanol with $H_2S$. On catalysts without strong proton centres on the surface, the coordination of methanol to the paired centres is probable: the oxygen atom is coordinated to a proton or a Lewis acid centre while the hydrogen atom of the OH methanol group is coordinated to a basic centre to form a methoxide group at the surface. Literature indicates then that thiolation reaction takes place with participation of surface methoxide groups and activated hydrogen sulphide on both acid and basic catalysts whose performances are governed by the strength of the acidic and basic sites. It is reported that on catalysts with paired acid–base centres, $H_2S$ could dissociate leading to HS groups formation and to an increasing rate for methanethiol formation. No study has discussed in details what was the optimum ratio of acidic and basic sites; however, the fact that paired acid–base centres involved in the mechanism of thiolation reaction suggests an optimal ratio equal to 1. The isopropanol decomposition test suggested that HapE-$CO_3$ could have close numbers of acidic and basic sites, but, it presented a lower conversion than Hap-Na-$CO_3$ possessing more acidic sites than basic ones. Thus, it seems that the ratio between acidic and basic sites could also influence the catalytic performance. In this case, catalytic performances of Hap-Na-$CO_3$ can be explained both by the quantity of acidic and basic surface sites and by an optimal ratio for methanol catalytic reaction.

## 4. Conclusion

Hydroxyapatite based materials were synthesized with various Ca/P ratios. These materials presented acidic and basic sites related to their Ca/P ratio. Addition of carbonate or sodium ions to the apatitic structure allowed to enhance and to adjust both acidic and basic surface-properties leading to very efficient catalysts in thiolation reaction of methanol. The best catalytic result was obtained using a slightly Ca-deficient Hap modified by $Na^+$ and $CO_3^{2-}$ ions.

## Acknowledgement

This work was financially supported by the Hubert Curien VOLUBILIS program between France and Morocco (MA/06/145).

## References

[1] E. Cadot, M. Lacroix, M. Breysse, E. Arretz, J. Catal. 164 (1996) 490.
[2] H.O. Folkins, E.L. Miller, Ind. Eng. Chem. Des. Dev. 1 (1962) 271.
[3] A.V. Mashkina, E.A. Paukshtis, V.N. Yakovleva, React. Kinet. Catal. Lett. 29 (1988) 514.
[4] A.V. Mashkina, E.A. Paukshtis, V.N. Yakovleva, G.V. Timofieeva, React. Kinet. Catal. Lett. 30 (1989) 1239.
[5] M. Ziolek, J. Kujawa, O. Saur, J.C. Lavalley, J. Phys. Chem. 97 (1993) 9761.
[6] A. El Ouassouli, S. Ezzemouri, M. Lakhdar, A. Ezzamarty, J. Leglise, J. Chim. Phys. 96 (1999) 1212.
[7] N. Elazarifi, A. Ezzamarty, J. Leglise, L.C. de Ménorval, C. Moreau, Appl. Catal. A: Gen. 267 (2004) 235.
[8] T. Tsuchida, J. Kubo, T. Yoshioka, S. Sakuma, T. Takeguchi, W. Ueda, J. Catal. 259 (2008) 183.
[9] D. Haffad, A. Chambellan, J.C. Lavalley, J. Mol. Catal. A: Chem. 168 (2001) 153.
[10] S.J. Joris, C.H. Amberg, J. Phys. Chem. 75 (1971) 3172.
[11] E.E. Berry, Bull. Soc. Chim. Fr. 1765 (1968) 70.
[12] S. Raynaud, E. Champion, D. Bernache-Assollant, P. Thomas, Biomaterials 23 (2002) 1065.
[13] B. Aellach, A. Ezzamarty, J. Leglise, C. Lamonier, J.-F. Lamonier, Catal. Lett. 135 (2010) 197.
[14] J.C. Elliott, Structure and Chemistry of the Apatites and Other Calcium Orthophosphates, Elsevier, Amsterdam, 1994.
[15] M. Achchar, C. Lamonier, A. Ezzamarty, M. Lakhdar, J. Leglise, E. Payen, C. R. Chim. 12 (2009) 671.
[16] G. Bonel, Ann. Chim. 7 (1972) 65.
[17] J.C. Elliott, G. Bonel, J. Appl. Crystallogr. 13 (1980) 618.
[18] J.C. Labarthe, G. Bonel, Ann. Chim. 8 (1973) 289.
[19] S. Padilla, I. Izquierdo-Barba, M.Ã. Vallet-Reg, Chem. Mater. 20 (2008) 5942.
[20] S.C. Liou, S.Y. Chen, H.Y. Lee, J.S. Bow, Biomaterials 25 (2004) 189.
[21] S. Kannan, J.M.G. Ventura, A.F. Lemos, A. Barba, J.M.F. Ferreira, Ceram. Int. 34 (2008) 7.
[22] A. Krajewski, M. Mazzochi, P.L. Buldini, A. Ravaglioli, A. Tinti, P. Taddei, C. Fagnano, J. Mol. Struct. 744 (2005) 221.
[23] S. Kannan, I.A.F. Lemos, J.H.G. Rocha, J.M.F. Ferreira, J. Solid State Chem. 178 (2005) 3190.
[24] M.E. Fleet, X. Liu, Biomaterials 28 (2007) 916.
[25] A. Antonakos, E. Liarokapis, T. Leventouri, Biomaterials 28 (2007) 3043.
[26] T. Tsuchida, J. Kubo, T. Yoshioka, S. Sakuma, T. Takegushi, W. Ueda, J. Catal. 259 (2008) 163.
[27] A.V. Mashkina, Russ. Chem. Rev. 64 (2) (1995) 1131.